

TEMPORAL POWER SPECTRUM OF SCATTERED ELECTROMAGNETIC WAVES IN THE EQUATORIAL TERRESTRIAL IONOSPHERE

GIORGI JANDIERI^{1*}, AKIRA ISHIMARU², NIKA TUGUSHI³ AND NINO MCHEDLISHVILI⁴

Abstract. Statistical characteristics of the temporal spectrum of scattered ordinary and extraordinary electromagnetic waves in the equatorial region of the conductive terrestrial ionosphere are investigated by using the stochastic transport equation for a frequency fluctuation, applying the geometrical optics approximation. The broadening of the temporal spectrum and the shift of its maximum involve the velocity of a turbulent plasma flow and the anisotropic parameters of electron density irregularities. Second-order statistical moments of electromagnetic waves do not depend on the absorption sign and are valid for both active and absorptive random media. The frequency of the turbulent pulsations and the conductivity of the ionospheric plasma have a substantial influence on the evaluation of the spectrum's varying propagation distances. A new double-humped effect in the temporal spectrum has been revealed for the ordinary wave at different anisotropy factors and the inclination angle of elongated plasmonic structures. Numerical calculations are carried out with the use of experimental data. Investigations of space-time fluctuations of electromagnetic wave radiation are of essential interest for radio astronomy and atmospheric physics.

1. INTRODUCTION

Many papers are devoted to the theoretical investigations and observations of the statistical characteristics of scattered radiation in turbulent plasma [5,7,19,20]. The analysis of the statistical properties of small-amplitude electromagnetic waves that have passed in a turbulent collision-magnetized plasma is very important in many practical applications associated with both natural and laboratory plasmas. In [8–11,13,15], peculiarities of the spatial spectrum of scattered electromagnetic waves in the F-region of the polar ionosphere were considered when applying the complex geometrical optics approximation and the modified smooth perturbation method. It was shown that the spatial-temporal fluctuations of electron density, the external magnetic field, anisotropy, and the angle of inclination of elongated irregularities relative to the geomagnetic lines of forces may lead to the amplification of the intensity of the frequency fluctuations of scattered electromagnetic waves in the collision magnetized plasma. Multiple scattered effects of waves are revealed more strongly at large scales with slowly varying time irregularities when the secondary waves with close frequencies propagate in a narrow spatial angle near the direction of the initial wave. Currently, the equatorial ionosphere is of great interest. The statistical characteristics of scattered electromagnetic waves in this region have not been considered until now. Ionospheric conductivity is one of the main parameters having substantial influence on plasma dynamics and transport mechanisms during waves propagation in the terrestrial ionosphere. In reality, inhomogeneous media randomly vary both in space and in time. Harmonic waves scattered over these irregularities become nonharmonic. Spectral lines become broad. Generally, the propagation of a wave with a complex spectral structure continuously changes its spectrum. The features of the temporal spectrum in the polar region of the terrestrial ionosphere have been considered in [14].

In this paper, we study for the first time the evaluation of the temporal spectrum of scattered ordinary (O-wave) and extraordinary (E-wave) electromagnetic waves in the equatorial ionosphere with a slowly varying position and time electron density irregularities using the four-dimensional WKB (Wentzel–Kramers–Brillouin) method. We investigate the influence of the absorption on the statistical characteristics of the wave in the turbulent collision-conductive magnetized plasma by using

2020 *Mathematics Subject Classification.* 26A33, 42B20.

Key words and phrases. Statistical moments; Electromagnetic waves; Turbulence; Temporal spectrum; Ionospheric irregularities; Conductivities.

*Corresponding author.

the stochastic transfer equation for the complex frequency based on the WKB method. The broadening and shifting of the maximum of the temporal spectrum include the direction of an external magnetic field, plasma velocity, ionospheric conductivities, the anisotropy factor of electron density irregularities and the inclination angle of elongated plasmonic structures with respect to the geomagnetic lines of forces. The problem is formulated in Section 2, where the second-order statistical moments describing the broadening phenomenon of the temporal spectrum and the shift of its maximum are derived by applying the eikonal equation and the stochastic transport equation for a complex frequency. In Section 3, the numerical results are presented with discussions based on the Gaussian correlation function of electron density irregularities containing anisotropic parameters of elongated plasmonic structures and the velocity of plasma flow as applied to the experimental data. Some conclusions and discussions are given in Section 4.

2. METHODS

2.1. Statistical moments of the temporal spectrum. Asymptotic and integrated methods are traditional instruments for studying the propagation of electromagnetic waves in various media. The method describing the mechanism of a short (2-40 MHz) radiowave propagation in the Earth ionosphere, which is the most developed and proven both theoretically and experimentally, is the geometrical optics approximation describing wave fields in a smoothly inhomogeneous medium with spatial-temporal irregularities [7, 17, 20]. In the case of ionospheric propagation, the following inequality is usually satisfied: $l \gg \lambda$ (λ is the wavelength of an incident wave). This inequality implies that only forward scattering is important in the random scattering process, and the WKB solution is valid for wave propagation. The phase satisfying the eikonal equation for each normal wave can be written as $c^2 k^2 = \omega^2 N^2(\omega, \mathbf{k}, n)$, where $\mathbf{k}(\mathbf{r}, t) = -\nabla\varphi$, $\omega(\mathbf{r}, t) = \partial\varphi/\partial t$ are the local wave vector and the frequency, respectively, which are the slowly varying functions of position and time; $n(\mathbf{r}, t)$ is a fluctuating component of the electron density of a turbulent plasma at the point \mathbf{r} ; $N^2(\omega, \mathbf{k})$ is the complex refraction index of a normal wave, c is the speed of light.

Statistical analysis of a phase and its derivatives on the basis of the eikonal equation is generally difficult, especially in a non-stationary medium, when $\omega(\mathbf{r}, t)$ is one of unknown quantities. In the quasi-monochromatic small-angle approximation, using the smoothness of the electron density variations $n(\mathbf{r}, t) = n_0 + n_1(\mathbf{r}, t)$, $|n_1| \ll n_0$, the first term is a constant density component and the second one is a random function of the spatial coordinates describing electron density fluctuations. Taking into account the index of refraction complexity $N(\mathbf{r}, t) = N_0(\mathbf{r}, t) - iN_1(\mathbf{r}, t)$, we can investigate statistical moments of the frequency fluctuations of a scattered electromagnetic wave in the equatorial ionosphere. The imaginary component of the index of refraction in the inhomogeneous anisotropic conductive plasma within the framework of the complex geometrical optics approximation is connected with a complex wave vector. The real part of this vector is connected with the plasma inhomogeneity and the refraction of waves, whereas the complex part of the inhomogeneous wave ($im\mathbf{k} \neq 0$) describes the evolution of inhomogeneous waves, including diffraction.

Consider the case in which the external magnetic field is directed along the Y-axis. In this case, the components of the complex permittivity tensor:

$$\begin{aligned} \tilde{\varepsilon}_{xx} = \tilde{\varepsilon}_{zz} = \varepsilon_{\perp} - i(\tilde{\sigma}_{\perp} + sg); \tilde{\varepsilon}_{xz} = -s\alpha\delta + i(\tilde{\sigma}_H + \alpha); \tilde{\varepsilon}_{yy} = (\varepsilon_{\perp} + p_0u) - i(\tilde{\sigma}_{\parallel} + sv); \\ \tilde{\varepsilon}_{xx} = \tilde{\varepsilon}_{zz}; \tilde{\varepsilon}_{zx} = -\tilde{\varepsilon}_{xz}; \varepsilon_{xy} = \varepsilon_{yx} = \varepsilon_{yz} = \varepsilon_{zy} = 0. \end{aligned}$$

Here

$$\begin{aligned} p_0 &= v/(1-u); \\ g &= p_0(1+u)/(1-u); \delta = 2/(1-u); g_1 = (3-u)/(1-u); \alpha = p_0\sqrt{u}; \\ v(\mathbf{r}) &= \omega_p^2(\mathbf{r})/\omega^2, u = (eH_0/m_e c\omega)^2 \end{aligned}$$

are the plasma frequency $\omega_p(\mathbf{r}) = [4\pi N_e(\mathbf{r})e^2/m_e]^{1/2}$ and the electron gyrofrequency, respectively. Normalized conductivity tensor $\tilde{\sigma} = 4\pi\hat{\sigma}/k_0c$ of ionospheric plasma for the equatorial latitude [1]

contains Hall's σ_H , Pedersen σ_{\perp} and longitudinal σ_{\parallel} conductivities:

$$\begin{aligned}\sigma_H &= e^2 n_e \left(\frac{\omega_e}{m_e(\nu_e^2 + \omega_e^2)} - \frac{\omega_i}{m_i(\nu_{in}^2 + \omega_i^2)} \right), \\ \sigma_{\perp} &= e^2 n_e \left(\frac{\nu_e}{m_e(\nu_e^2 + \omega_e^2)} + \frac{\nu_i}{m_i(\nu_{in}^2 + \omega_i^2)} \right), \\ \sigma_{\parallel} &= e^2 n_e \left(\frac{1}{m_e \nu_e} + \frac{1}{m_m \nu_{in}} \right).\end{aligned}$$

Here $k_0 = \omega_0/c$, m_e and e are the mass and charge of an electron, $\nu_e = \nu_{en} + \nu_{in}$ is the effective collision frequency of electrons with other plasma particles; ω_e and ω_i are the angular gyrofrequencies of an electron and ion, respectively.

The complex refractive index N of the conductive collision ionospheric magnetized plasma in the equatorial region of the terrestrial atmosphere at $s \neq 0$, $\tilde{\sigma}_y \neq 0$ and $s \ll \varepsilon_{ij}$, $\tilde{\sigma}_{ij}$ is written as follows:

$$N(n, \omega) = N_0(n_0, \omega) - iN_1(n, \omega),$$

where

$$\begin{aligned}N_0 &= \sqrt{(r + \Gamma_0)/2}; \quad N_1 = \sqrt{(r - \Gamma_0)/2}; \quad r = \sqrt{\Gamma_0^2 + \Gamma_1^2}; \\ \Gamma_0 &= 1 - 2(T_1 T_0 - T_2 \psi_2)(T_1^2 + T_2^2)^{-1}; \quad \Gamma_1 = 2(T_2 T_0 + T_1 \psi_2)/(T_1^2 + T_2^2)^2; \\ T_1 &= A \pm D_1; \quad T_2 = R_1 \pm D_2; \quad D_1 = \sqrt{(r_1 + B)/2}; \quad r_1 = \sqrt{B^2 + C^2}; \\ D_2 &= \sqrt{(r_1 - B)/2}; \quad \psi_1 = \Lambda_1(\sin^2 \theta - \varepsilon_{\parallel}) + \tilde{\sigma}_{\parallel} \tilde{\sigma}_{\perp}(1 + \cos^2 \theta - 2\varepsilon_{\perp} \varepsilon_{\parallel}); \quad C = \psi_6 - \psi_8; \\ \Lambda_1 &= \tilde{\sigma}_{\perp}^2 + \tilde{\sigma}_H^2 + 2\tilde{\alpha} \tilde{\sigma}_H, \quad \psi_2 = \tilde{\sigma}_{\perp} \sin^2 \theta + \tilde{\sigma}_{\parallel} \cos^2 \theta - \Lambda_2 + 2\varepsilon_{\parallel} \varepsilon_{\perp} \tilde{\sigma}_{\perp} + \tilde{\sigma}_{\parallel}(\varepsilon_{\perp}^2 - \tilde{\alpha}^2 - \Lambda_1); \\ \Lambda_2 &= 2\varepsilon_{\perp} \tilde{\sigma}_{\perp} \sin^2 \theta + (\varepsilon_{\parallel} \tilde{\sigma}_{\perp} + \varepsilon_{\perp} \tilde{\sigma}_{\parallel})(1 + \cos^2 \theta); \quad c = (1 - \nu)[(1 - \nu)^2 - u]/(1 - u); \\ b &= [2(1 - \nu)^2 - 2u + \nu u(1 + \cos^2 \theta)](1 - u)^{-1}; \quad A = p_0[2(1 - \nu) - \sin^2 \theta]; \\ T_0 &= p_0 \nu(1 - \nu) + \psi_1; \quad \alpha = 1 - p_0(1 - u \cos^2 \theta); \quad \psi_3 = \Lambda_1 \sin^2 \theta + \tilde{\sigma}_{\parallel} \tilde{\sigma}_{\perp}(1 + \cos^2 \theta); \\ \psi_4 &= \Lambda_2 - 2(\tilde{\sigma}_{\perp} \sin^2 \theta + \tilde{\sigma}_{\parallel} \cos^2 \theta); \quad \psi_6 = 2\Lambda_2[\Lambda_1 \sin^2 \theta + \tilde{\sigma}_{\parallel} \tilde{\sigma}_{\perp}(1 + \cos^2 \theta) - b]; \\ B &= p_0^2[u^2 \sin^4 \theta + 4u(1 - \nu)^2 \cos^2 \theta] + (\psi_5 - \psi_7); \\ \psi_5 &= \Lambda_1^2 \sin^4 \theta + \tilde{\sigma}_{\parallel}^2 \tilde{\sigma}_{\perp}^2(1 + \cos^2 \theta)^2 - \Lambda_2^2 - 2b[\Lambda_1 \sin^2 \theta + \tilde{\sigma}_{\parallel} \tilde{\sigma}_{\perp}(1 + \cos^2 \theta)] \\ &\quad + 2\Lambda_1 \tilde{\sigma}_{\parallel} \tilde{\sigma}_{\perp} \sin^2 \theta(1 + \cos^2 \theta); \\ \Lambda_3 &= (\tilde{\sigma}_{\perp} \sin^2 \theta + \tilde{\sigma}_{\parallel} \cos^2 \theta)[2\varepsilon_{\parallel} \varepsilon_{\perp} \tilde{\sigma}_{\perp} + \tilde{\sigma}_{\parallel}(\varepsilon_{\perp}^2 - \tilde{\alpha} - \Lambda_1)]; \\ \psi_7 &= 4[\Lambda_3 + \alpha \varepsilon_{\parallel}(\Lambda_1 + 2\varepsilon_{\perp} \tilde{\sigma}_{\parallel} \tilde{\sigma}_{\perp})]; \\ \psi_8 &= \alpha[2\varepsilon_{\parallel} \varepsilon_{\perp} \tilde{\sigma}_{\perp} + \tilde{\sigma}_{\parallel}(\varepsilon_{\perp}^2 - \tilde{\alpha} - \Lambda_1)] + (\tilde{\sigma}_{\perp} \sin^2 \theta + \tilde{\sigma}_{\parallel} \cos^2 \theta)[c - \varepsilon_{\parallel}(\Lambda_1 + 2\varepsilon_{\perp} \tilde{\sigma}_{\parallel} \tilde{\sigma}_{\perp})].\end{aligned}$$

The upper sign corresponds to the O-wave, the lower sign to the E-wave; θ is the angle between the \mathbf{H}_0 and \mathbf{k}_0 vectors. For the collisionless and nonconductive turbulent plasma, we obtain the well-known formula [6].

As is well known [5, 7, 19, 20] during the propagation of a radio signal in a randomly inhomogeneous nonstationary plasma, the Doppler shift is small compared to the transmitter frequency, and the spectrum broadens. The quantitative estimation of the frequency fluctuations is important, as far as the broadening of a spectrum limits the resolution of Doppler's method in study the structure of the receiving signal. On the other hand, by measuring the width of the Doppler spectrum, it is possible to solve the reverse task by receiving information about the statistical properties of plasma. The ratios connecting changes in frequency with the parameters of moving plasma irregularities make it necessary to apply statistical methods as a tool for the solution of direct and reverse problems of radiowave propagation in a non-stationary plasma.

For an arbitrary spatial-temporal dispersion in the geometrical optics approximation, neglecting polarization effects, the wave frequency satisfies the stochastic differential transport equation [4, 18]:

$$\left(\frac{\partial}{\partial t} + (\mathbf{u}\nabla)\right)\omega = -\frac{\omega\mathbf{u}}{c} \sum \frac{\partial N}{\partial p_i} \frac{\partial p_i}{\partial t}, \quad (2.1)$$

where $N(\omega, p_i) = ck/\omega$ is the complex index of refraction, $\mathbf{u} = (d\omega/d\mathbf{k})_{p_i}$ is the group velocity of the wave, p_i is an arbitrary parameter characterizing turbulent plasma. We assume that in a zero-order approximation, a plane wave propagates in the y -direction. The eikonal equation describes virtual ray trajectories that can be measured experimentally. Ray paths deviate toward an increase in the index of refraction. Radiowaves, propagating in the lower ionosphere, have a ray path that deviates towards the Earth; during the propagation of these waves through the upper ionosphere, the ray path deviates in the opposite direction.

The variation of the frequency fluctuations is one of the important spectral characteristics specified for nonstationary media. It determines the broadening of the temporal spectrum in the turbulent plasma and can be found by measurements of the phase. Applying equation (2.1) to the first order approximation, the frequency fluctuation satisfies the stochastic transport differential equation

$$\frac{\partial\omega_1}{\partial y} + \frac{q_0}{c}(1 + i\psi_0)\frac{\partial\omega_1}{\partial t} = -k_0(\psi_1 + i\psi_2)\frac{\partial n_1}{\partial t}, \quad (2.2)$$

where $q_0 = N_0 + \omega_0 \partial N_0/\partial\omega$, $\psi_0 = (N_1 + \omega_0 \partial N_1/\partial\omega_0)/q_0$; $\psi_1 = \partial N_0/\partial n_0$; $\psi_2 = \partial N_1/\partial n_0$;

$$\psi_1 = \frac{1}{4N_0} \left[\left(\frac{\Gamma_0}{r_1} + 1 \right) \frac{\partial\Gamma_0}{\partial n_0} + \frac{1}{r_1} \Gamma_1 \frac{\partial\Gamma_1}{\partial n_0} \right],$$

$$\psi_2 = \frac{1}{4N_1} \left[\left(\frac{\Gamma_0}{r_1} - 1 \right) \frac{\partial\Gamma_0}{\partial n_0} + \frac{1}{r_1} \Gamma_1 \frac{\partial\Gamma_1}{\partial n_0} \right]$$

$r_1 = (\Gamma_0^2 + \Gamma_1^2)^{1/2}$, $V_{gr} = c[\partial(N\omega)/\partial\omega]^{-1}$, is the group velocity of an unperturbed wave propagating along the y -axis in a conductive collision absorptive magnetized plasma. The direction of a group speed and a wave vector cannot coincide in an anisotropic absorbing plasma. The energy flux of a wave propagating along the ray path at each point coincides with the group velocity V_{gr} . In the absence of spatial dispersion, it also coincides with the direction of an average Poynting vector. However, the conductivity of plasma may lead to the opposite directions of the Poynting vector and the wave vector, and hence, the group velocity will become negative.

For the solution of equation (2.2), we apply the Fourier transform

$$\omega_1(\mathbf{r}, t) = \int_{-\infty}^{\infty} d\nu \Omega(\mathbf{r}, \nu) \exp(i\nu t).$$

We suppose that randomly varying electron density irregularities having characteristic spatial scale l are located in the slab: $0 < y < L$ and the fluctuations of the wave parameters are absent at $y < 0$ at the observation point beyond the slab: $y > L$, we obtain

$$\Omega(\boldsymbol{\rho}_\perp, y, \nu) = k_0\nu(\psi_2 - i\psi_1) \exp\left[\frac{\nu}{c}q_0(\psi_0 - i)y\right]$$

$$\times \int_0^L d\zeta n_1(\boldsymbol{\rho}_\perp, \zeta, \nu) \exp\left[\frac{\nu}{c}q_0(-\psi_0 + i)\zeta\right];$$

here, $\boldsymbol{\rho}_\perp = \{x, z\}$ It is evident that the instantaneous local frequency randomly varies in space and time, while these fluctuations at the observation point \mathbf{r} and the moment t are created due to a multiple interaction of a wave with all irregularities laying on a path of wavy perturbations, and are determined by chaotic electron density fluctuations at the time moments when wavy perturbations pass through them with a group velocity $V_{gr} = c(1 - i\psi_0)/q_0$. Electronic density varies randomly with both position and time. Nonstationarity is caused by the movement of a plasma stream and the temporal pulsations of electron density fluctuations. The monochromatic waves scattered by electron density fluctuations become nonmonochromatic. Spectral lines become broad. Generally,

waves with a complex spectral structure continuously change the spectrum. In experiments observing the scattering of electromagnetic waves with different frequencies, the receiving signal has a Doppler shift and a widened spectrum. They are caused by the convection of scattered irregularities and the temporal fluctuations of electron density.

The second-order statistical moments of the frequency fluctuation of scattered electromagnetic waves in the equatorial region of the terrestrial ionosphere at $L \gg l$ and in a weakly absorptive plasma $q_0 < 1$ can be written as follows:

$$\Delta_1 = \pi (\psi_1^2 + \psi_2^2) \frac{ck_0^2}{q_0\psi_0} \int_{-\infty}^{\infty} d\nu \nu \int_{-\infty}^{\infty} d\mathbf{k}_\perp W_n(\mathbf{k}_\perp, k_y, \nu),$$

$$\left\{ \exp\left(2\frac{q_0\psi_0}{c}y\nu\right) - \exp\left[2\frac{q_0\psi_0}{c}(y-L)\nu\right] \right\} \exp(i\mathbf{k}_\perp \boldsymbol{\rho}_\perp), \quad (2.3)$$

$$\Delta_2 = \pi k_0^2 L (\psi_1^2 - \psi_2^2) \int_{-\infty}^{\infty} d\nu \nu^2 \int_{-\infty}^{\infty} d\mathbf{k}_\perp W_n(\mathbf{k}_\perp, k_y, \nu) \exp(i\mathbf{k}_\perp \boldsymbol{\rho}_\perp), \quad (2.4)$$

where the pointed brackets indicate ensemble average, the asterisk complex conjugate, $\mathbf{k}_\perp = (k_x, k_z)$

$$W_n(\mathbf{k}_\perp, k_y, \nu) = \frac{1}{(2\pi)^4} \int_{-\infty}^{\infty} d\rho_\perp \int_{-\infty}^{\infty} d\rho_y \int_{-\infty}^{\infty} d\tau V_n(\rho_\perp, \rho_y, \tau) \exp(i\mathbf{k}_\perp \boldsymbol{\rho}_\perp + ik_y \rho_y - i\nu\tau)$$

is an arbitrary correlation function of electron density fluctuations, $k_y = \nu q_0/c$. The temporal spectrum is determined by the formula

$$\Delta = \Delta_1 + \Delta_2.$$

Broadening of the temporal power spectrum $\Delta \equiv \langle \omega_1^2 \rangle / \omega_0^2$ can be easily measured by experiment; $\Delta_1 \equiv \langle \omega_1 \omega_1^* \rangle / 2\omega_0^2$, $\Delta_2 \equiv \text{Re} \langle \omega_1 \omega_2 \rangle / 2\omega_0^2$. As the violation of the field coherence in medium with large-scale irregularities is caused by the phase fluctuations, we can suggest that the variance of the wave frequency $\langle \omega_1^2 \rangle$ keeps its sense at diffraction, too. At those distances, where the absorption becomes essential, the second term in equation (2.4) is much less than the first one. The fact that the violation of coherence of the field in the media with large-scale irregularities is connected generally with phase fluctuations gives the grounds to consider that the dispersion of frequency $\langle \omega_1^2 \rangle$ of a wave keeps the sense in the presence of diffraction, as well. Diffraction may exert the influence on the variance of frequency fluctuations only in Fraunhofer's zone with respect to the spatial scale of irregularities l (at $(y/k_0 l^2) \gg 1$). Physically, this can be explained from the fact that the waves scattered under a big angle attenuate faster along the y axis.

3. RESULTS

3.1. Numerical calculations. Experimental results concerning the features of large-scale artificial plasma density irregularities induced in the ionospheric region by high-power radiowaves using the SURA heating facility were presented in [3]. Transverse scale of these irregularities l_\perp with respect to the geomagnetic field varies from meters up to tens of kilometers. Large-scale plasma irregularities due to electron density variation along the sight beam on the satellite may have the following sizes: $l_{||} = 30 \text{ km}$, the drift velocity $30 \div 35 \text{ m/s}$. It was revealed that the heating of ionospheric plasma by powerful radiowaves causes the generation of artificial large-scale ionospheric irregularities from several tens to one hundred kilometers, which can influence the propagation of radiowaves in different frequency bands.

Observations (Tbilisi, $41^\circ 43\text{N}$) of drift small-scale irregularities in the ionospheric F-region show [16] that they have elliptic form, the ratio of axes basically varies from 1 to 3. Anisotropy axis is mainly oriented along the geomagnetic field of lines. The drift of small-scale irregularities mainly has S-W direction. The most probable values of drift velocity are in the range of 40-100 meter/sec. Small-scale irregularities with Gaussian spectrum are responsible for polarization fluctuations at frequencies of 20-50 MHz.

Data obtained from spaced receiver measurements made at Kingston, Jamaica (during the periods August 1967–January 1969 and June 1970–September 1970) show that the irregularities between heights of 153 and 617 km causing the scintillation of signals from the moving earth satellites (BE–B and BE–C) are closely aligned along the magnetic field lines in the F–region [2]. The dip angle of the irregularities with respect to the field lines was within 16° . The anisotropic spectral features in the F–region are defined for the Gaussian and power-law spectra. For the F region, large scale irregularities ($\sim 10km$) become unstable and dissipate their energy by generating small-sized irregularities, as is the case in turbulence. In the equatorial region, the large-scale irregularities are most likely produced by a convective electric field.

We use the spatial-temporal spectrum of electron density irregularities [12]:

$$V_n(\mathbf{k}, \nu) = \frac{\sigma_n^2}{16\pi^2} \frac{l_{\parallel}^3}{\chi^2 \left[1 + l_{\perp}^2 (k_x^2 + k_y^2) + l_{\parallel}^2 k_z^2 \right]^{p/2}} \times \exp \left(-\frac{k_x^2 l_{\perp}^2}{4} - t_0 \frac{k_y^2 l_{\parallel}^2}{4} - t_1 \frac{k_z^2 l_{\parallel}^2}{4} - t_2 \frac{\nu^2 T^2}{4} \right); \quad (3.1)$$

here,

$$\begin{aligned} p_2 &= (\sin^2 \gamma_0 + \chi^2 \cos^2 \gamma_0) / \chi^2; \quad \alpha_1 = 1 + \eta^2 (\bar{l}/l_{\perp})^2; \quad \bar{l} = l_{\perp} l_{\parallel} \left(l_{\perp}^2 \sin^2 \gamma_0 + l_{\parallel}^2 \cos^2 \gamma_0 \right)^{-1/2}; \\ \eta &= V_0 T / l_{\parallel}; \quad G_0 = [1 - \eta / (2\alpha_1)]^{1/2}; \quad G_1 = (\chi^2 - 1) \eta \sin \gamma_0 \cos \gamma_0 / \chi^2 p_2; \\ t_0^2 &= \alpha_0 - 1 / (p_2 \chi^2); \quad t_1 = b_0 + p_2 G_2 (l_{\parallel} / cT) q_0 / G_0^2; \quad b_0 = (G_1 / \alpha_1) - p_2 G_2 G_3 / G_0^2; \\ t_2 &= c_0 + p_2 q_0^2 (l_{\parallel} / cT)^2 / G_0^2; \quad c_0 = (1 / \alpha_1) + p_2 G_3^2 / G_0^2; \quad G_3 = \eta / (\alpha_1 p_2); \\ G_2 &= (\chi^2 - 1) \sin \gamma_0 \cos \gamma_0 / (\sin^2 \gamma_0 + \chi^2 \cos^2 \gamma_0) - (\eta G_1 / \alpha_1 p_2). \end{aligned}$$

The anisotropy of electron density irregularities is a result of the diffusion processes in the ionosphere. The shape of irregularities depends on the diffusion coefficients in the field-aligned and field-perpendicular directions. The ellipsoid is characterized by two parameters: the anisotropy factor for the irregularities the ratio of ellipsoidal axes $\chi = l_{\parallel} / l_{\perp}$ (ratio of longitudinal and transverse linear scales of plasma irregularities with respect to the external magnetic field); γ_0 is the inclination angle of elongated ionospheric plasmonic structures with respect to the magnetic lines of force; $T = l / V$ is the characteristic temporal scale of electron density fluctuations. The drift velocity of plasma inhomogeneities exceeds that of the temporal pulsations changing their shapes. If $V_0 = 0$, we obtain [8–10, 12]. Substituting (3.1) into equations (2.3) and (2.4), we obtain the broadening of the temporal spectrum of scattered ordinary and extraordinary waves in the equatorial ionosphere:

$$\begin{aligned} \Delta_1 &= \frac{\sigma_n^2}{8\pi} (\psi_1^2 + \psi_2^2) \frac{cT}{l_{\parallel}} \frac{\xi^2}{q_0 \psi_0 \sqrt{p_1}} \frac{1}{(\omega_0 T)^2} \int_{-\infty}^{\infty} d\eta \frac{\eta}{\left[1 + \left(1 + \frac{4}{\chi^2} \frac{p_3^2}{p_1^2} \right) \left(\frac{l_{\parallel}}{cT} \right)^2 q_0^2 \eta^2 \right]^2} \\ &\times \exp \left\{ -\frac{\eta^2}{4} \left[1 + 4q_0^2 \left(\frac{l_{\parallel}}{cT} \right)^2 \left(\frac{p_2}{4} - \frac{p_3^2}{p_1^2} \right) \right] \right\} \\ &\times \left\{ \exp \left[2q_0 \psi_0 \left(\frac{l_{\parallel}}{cT} \right) \frac{L}{l_{\parallel}} \frac{z}{L} \eta \right] - \exp \left[2q_0 \psi_0 \left(\frac{l_{\parallel}}{cT} \right) \left(\frac{z}{L} - 1 \right) \eta \right] \right\}; \\ \Delta_2 &= \frac{\sigma_n^2}{4} (\psi_1^2 - \psi_2^2) \frac{\xi^2}{\chi (\omega_0 T)^2 \sqrt{p_1}} \frac{L}{l_{\parallel}} \\ &\times \int_{-\infty}^{\infty} d\eta \frac{\eta^2}{\left[1 + \left(1 + \frac{4}{\chi^2} \frac{p_3^2}{p_1^2} \right) \left(\frac{l_{\parallel}}{cT} \right)^2 q_0^2 \eta^2 \right]^2} \exp \left(-\frac{\eta^2}{4} \right) \end{aligned}$$

According to the findings, when dumping is small on the wavelength but large on all lengths of a wave path, frequency fluctuations grow much faster than in a similar medium without absorption [4, 18]. This growth continues outside the layer containing irregularities (at $y > L$). It is essential to note that the statistical moment (9) does not depend on the sign of the parameter ψ_0 , i.e., the obtained results are valid for both an absorbing and an active media. The reason for this effect is that frequency perturbations in a medium with a complex refractive index are not only transferred along Y axes with a group velocity [18], but also amplified. Obviously, a similar effect will take place in a homogeneous medium with a complex refractive index for an incident frequency-modulated wave. The modulator in our case is a turbulent plasma layer.

Numerical calculations are carried out for an incident wave with a frequency of 3 MHz. Figure 1(a) depicts the temporal spectrum E-wave broadening as a function of the temporal parameter ν_0/ω_0 . In the plasma slab $y/L = 0.5$ with a varying anisotropic factor in the interval $3 \leq \chi \leq 10$, at $\gamma_0 = 5^\circ$, the spectrum broadens three times and its maximum is displaced to the left two times. Out of the slab, varying the parameter in the interval $1 \leq (y/L) \leq 20$, the spectrum broadening increases five times and its maximum is displaced to the left two times. Numerical calculations show that for the O-wave at $\chi = 7$ and $\gamma_0 = 8^\circ$, in the space interval $9 \leq (y/L) \leq 11$, the spectrum broadening increase six time and its maximum slightly changes.

Figure 1(b) shows the plots of the temporal power spectrum of a scattered E-wave in the equatorial region of the conductive magnetized turbulent plasma for the different inclination angle $1^\circ \leq \gamma_0 \leq 9^\circ$ of elongated electron density irregularities with respect to the geomagnetic lines of forces.

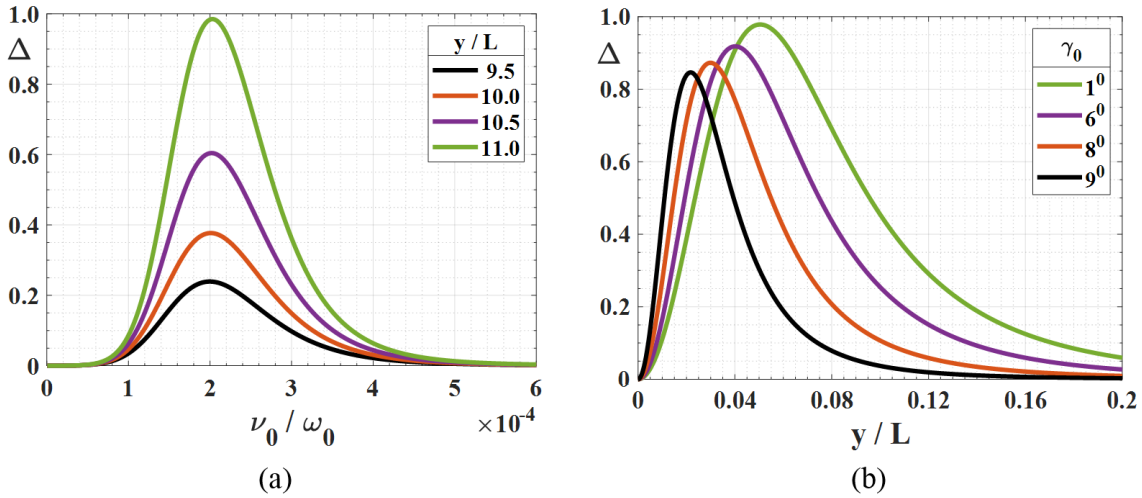


FIGURE 1. The broadening of the temporal spectrum and the shift of its maximum for E-wave vs dimensionless frequency and distance parameters.

Figure 1(a) illustrates the evaluation of the temporal spectrum for different anisotropy factor.

Figure 1(b) illustrates the evaluation of the temporal spectrum for different inclination angle of elongated ionospheric plasmonic structures with respect to the magnetic lines of force.

Varying anisotropy factor in the interval $3 \leq \chi \leq 12$, the spectrum broadens slightly; particularly, at $\chi = 3$, the spectrum maximum displaces to the left seven times, at $\chi = 6$ is displaced 16 times, at $\chi = 9$ -ten times.

Figure 2(a) illustrates the evaluation of the temporal spectrum for different anisotropy factor

Figure 2(b) illustrates the evaluation of the temporal spectrum for different anisotropy factor

Analyses show that at $2 \leq \chi \leq 14$ and $\gamma_0 = 4^\circ$, the spectrum broadens six times and its maximum shifts to the left four times. Figure 2(b) illustrates the behavior of the spectrum for different anisotropy

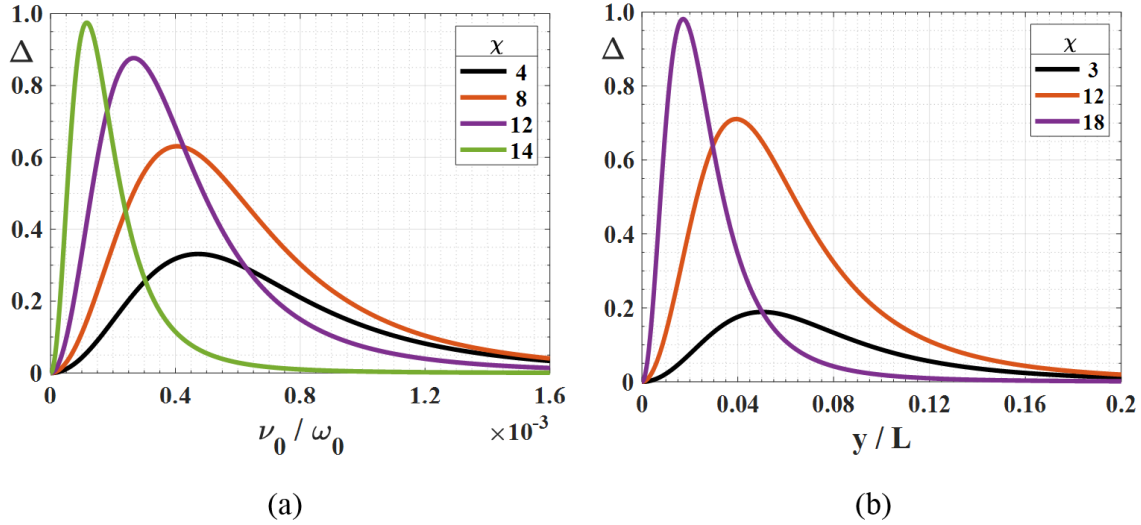


FIGURE 2. The broadening of the temporal spectrum at different anisotropy factors for E-wave.

factor. Analyses show that varying anisotropic parameter in the interval $3 \leq \chi \leq 18$ maximum, the broadening of the spectrum increases and maximum of the spectrum shifts to the left.

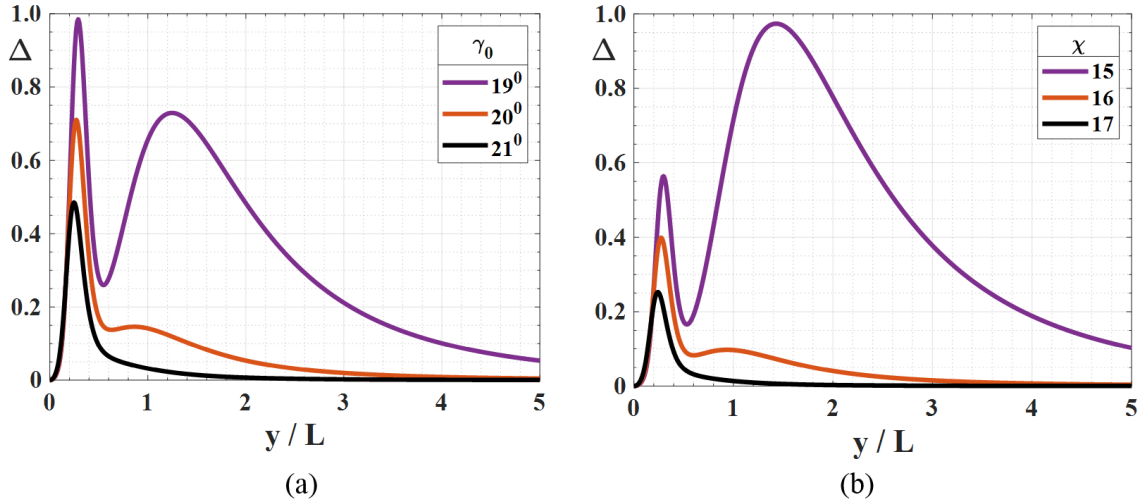


FIGURE 3. Evaluation of the temporal spectrum as a function of dimensionless distance parameter for O-wave.

Figure 3(a) illustrates the evaluation of the temporal spectrum for different inclination angle of elongated ionospheric plasmonic structures with respect to the magnetic lines of force.

Figure 3(b) illustrates the evaluation of the temporal spectrum for different anisotropy factor.

The curves describing the broadening of the temporal spectrum of O-wave in the turbulent ionospheric plasma at the anisotropy coefficient $\chi = 3$ varying distance $0 \leq (y/L) \leq 10.5$ are plotted in Figure 3 (a). Numerical calculations show that at $\gamma_0 = 17^\circ$, there arise two humps; broadening of the first hump is very small. At $\gamma_0 = 19^\circ$, these humps have the same width. Increasing the inclination angle up to $\gamma_0 = 21^\circ$, the second hump disappears. The same behavior of the curves is observed at $\chi = 6$, but the broadening of a second curve becomes substantially small at $\gamma_0 = 9^\circ$. Figure 3(b) illustrates the broadening and shift of the spectrum maximum of O-wave at $\gamma_0 = 3^\circ$ at

different anisotropy factor $15 \leq \chi \leq 17$. Numerical calculation show that two humps arise at $\chi = 14$ and disappear at $\chi = 17$. Similar to the previous case, increasing tilt angle γ_0 , there arise the humps in the temporal spectrum at small anisotropy factor, and the evaluation of the spectrum is the same.

4. CONCLUSION

Analytical calculations and numerical simulations of the temporal spectrum of scattered electromagnetic waves propagating in the equatorial ionosphere were carried out. For the first time, the index of refraction for this region of the terrestrial atmosphere has been obtained. Statistical characteristics of the temporal spectrum (broadening and displacement of its maximum) of scattered ordinary and extraordinary electromagnetic waves propagating in the conductive collision magnetized plasma are investigated in the geometrical optics approximation by using the stochastic transport equation for the frequency fluctuation.

Second-order statistical moments: The correlation function and the variance of the frequency fluctuations, characterized by the broadening of the temporal spectrum and the shift of its maximum, have been obtained for the arbitrary anisotropic correlation function of electron density fluctuations.

Numerical calculations are carried out for the anisotropic Gaussian spatial-temporal spectrum of electron density fluctuations containing anisotropic parameters characterizing turbulent ionospheric plasma: the external magnetic field, plasma velocity, anisotropy factor, and inclination angle of elongated plasmonic structures with respect to the lines of force of the geomagnetic field. Investigation shows that the anisotropy factor and the inclination angle of elongated plasmonic structures have a substantial influence on the broadening of the temporal power spectrum and the shift of the maximum of scattered O- and E-waves in the equatorial ionosphere. A new double-humped effect has been revealed to arise in the temporal spectrum of scattered O-wave in the equatorial region, and it is absent for E-wave. This effect is not observed in the polar ionosphere. Diffraction effects have the greatest influence on frequency variance in nonstationary plasma during longitudinal propagation, when absorption is essential.

Measurements of the statistical characteristics of scattered electromagnetic waves by satellite, ground-based radar systems, or meteorological-ionospheric stations give information about ionospheric plasma irregularities. The active use of electromagnetic waves in the short-wave band in antenna equipment for long-distance radio communication, radio navigation, radar location, and also studying the structure of an ionosphere, the upper atmosphere of Earth via remote sensing and radio tomography defines the relevance of a research.

ACKNOWLEDGEMENT

This work was supported by the Shota Rustaveli National Science Foundation of Georgia (SRNSFG), grant NFR-21-316 “Investigation of the statistical characteristics of scattered electromagnetic waves in the terrestrial atmosphere and application”.

REFERENCES

1. M. Aydoğdu, E. Güzel, A. Yeşil, O. Özcan, M. Canyılmaz, Comparison of the calculated absorption and the measured field strength of HF waves reflected from the ionosphere. *Nuovo Cimento C* **30** (2007), no. 3, 243–253.
2. A. A. Chen, G. S. Kent, Determination of the orientation of ionospheric irregularities causing scintillation of signals from earth satellites. *Journal of Atmospheric and Terrestrial Physics* **34** (1972), no. 8, 1411–1414.
3. V. L. Frolov, E. A. Shorokhova, V. E. Kunitsyn, E. S. Andreeva, A. M. Padokhin, Peculiarities of excitation of large-scale plasma density irregularities HF-induced by modification of the ionospheric F_2 region. *Izvestia VUZ, Radiofiz.* **58** (2015), no. 10, 797–810.
4. V. G. Gavrilenko, N. S. Stepanov, Statistical characteristics of waves in the chaotically media with spatial-temporal irregularities. *Izv. VUZ. Radiophysics* **20** (1987), 3–35.
5. B. N. Gershman, L. M. Erukhimov, Iu. Ia. Yashin, *Wave Phenomena in the Ionosphere and Space Plasma*. (Russian) Nauka, Moscow, 1984.
6. V. L. Ginzburg, *Propagation of Electromagnetic Waves in Plasma*. Translated from the Russian by Royer and Roger; edited by Walter L. Sadowski, D. M. Gallik. Gordon and Breach Science Publishers, Inc., New York, 1961.
7. A. Ishimaru, *Wave Propagation and Scattering in Random Media*. Reprint of the 1978 original. With a foreword by Gary S. Brown. IEEE/OUP Series on Electromagnetic Wave Theory. An IEEE/OUP Classic Reissue. IEEE Press, New York, 1997.

8. G. V. Jandieri, Double-Humped effect in the turbulent magnetized plasma. *PIER M* **48** (2016), 95–102.
9. G. V. Jandieri, Z. Diasamidze, I. Takidze, Second order statistical moments of the phase fluctuations of scattered radiation in the collision magnetized plasma. *CSC Athens*, 134–138, 2016.
10. G. V. Jandieri, A. Ishimaru, V. Jandieri, A. Khantadze, Z. Diasamidze, Model computations of angular power spectra for anisotropic absorptive turbulent magnetized plasma. *PIER* **70** (2007), 307–328.
11. G. V. Jandieri, A. Ishimaru, S. Banmali, B. Rawat, N. K. Tugushi, Peculiarities of the spatial power spectrum of scattered electromagnetic waves in the turbulent collision magnetized plasma. *PIER* **152** (2015), 137–149.
12. G. V. Jandieri, A. Ishimaru, B. Rawat, O. Kharshiladze, Zh. Diasamidze, Power spectra of ionospheric scintillations. *Advanced Electromagnetics* **6** (2017), no. 4, 42–51.
13. G. V. Jandieri, A. Ishimaru, B. Rawat, V. Gavrilenko, O. Kharshiladze, Statistical moments and scintillation level of scattered electromagnetic waves in the magnetized plasma. *Advanced Electromagnetics* **7** (2018), no. 3, 1–10.
14. G. V. Jandieri, A. Ishimaru, B. Rawat, N. K. Tugushi, Temporal spectrum of scattered electromagnetic waves in the conductive collision turbulent magnetized plasma. *Advanced Electromagnetics* **11** (2022), no. 1, 1–8.
15. G. V. Jandieri, N. N. Zhukova, I. G. Takidze, V. Jandieri, Statistical characteristics of scattered radiation in medium with spatial-temporal fluctuations of electron density and external magnetic field. *J. Electromagnetic Analysis and Application* **4** (2012), 243–251.
16. N. D. Kvavadze, Z. L. Liadze, N. V. Mosashvili, Z. S. Sharadze, The phenomenon of F-scattering and drift of small-scale irregularities at night low latitudes F-region of an ionosphere. *Geomagnetism and Aeronomy* **28** (1988), no. 1, 139–141.
17. Yu. A. Kravtsov, Yu. I. Orlov, *Geometrical Optics of Inhomogeneous Media*. (Russian) Nauka, Moscow, 1980.
18. Yu. A. Kravtsov, L. A. Ostrovsky, N. S. Stepanov, Geometrical optics of inhomogeneous and nonstationary dispersive media. *Proceedings IEEE* **62** (1974), no. 11, 1492–1510.
19. S. M. Rytov, Yu. A. Kravtsov, V. I. Tatarskii, *Principles of Statistical Radiophysics*. 3. Elements of random fields. Springer-Verlag, Berlin, 1989.
20. V. I. Tatarskii, *Wave Propagation in a Turbulent Medium*. Translated from the Russian by R. A. Silverman. McGraw-Hill Book Co., Inc., New York-Toronto-London, 1961.

(Received 21.11.2022)

¹INTERNATIONAL SPACE AGENCY GEORGIAN SOCIETY, GTU, TBILISI, GEORGIA

²DEPARTMENT OF ELECTRICAL ENGINEERING, UNIVERSITY OF WASHINGTON, SEATTLE, USA

³DEPARTMENT OF PHYSICS, TBILISI STATE UNIVERSITY, TBILISI, GEORGIA

⁴DEPARTMENT OF CONTROL SYSTEM, GEORGIAN TECHNICAL UNIVERSITY, TBILISI, GEORGIA

Email address: `george.jandieri@gtu.ge`

Email address: `ishimaru@u.washington.edu`

Email address: `nika.tughushi107@ens.tsu.edu.ge`

Email address: `nino.mchedlishvili@gtu.ge`